TELEOST CHLORIDE CELL
II. Autoradiographic Localization of Gill Na,K-ATPase in Killifish *Fundulus heteroclitus* Adapted to Low and High Salinity Environments

KARL J. KARNAKY, JR., LEWIS B. KINTER, WILLIAM B. KINTER, and CHARLES E. STIRLING

From the Mount Desert Island Biological Laboratory, Salsbury Cove, Maine 04672, and the University of Washington, Seattle, Washington 98105. Lewis B. Kinter's present address is the Department of Physiology, Harvard Medical School, Boston, Massachusetts 02115.

ABSTRACT

The specific binding and inhibitory action of [^{3}H]ouabain were employed to localize transport Na,K-ATPase in the euryhaline teleost gill, a NaCl-transporting osmoregulatory tissue in which both enzyme activity and transepithelial transport vary with environmental salinity. In killifish fully adapted to 10%, 100%, or 200% seawater, the gills were internally perfused and externally irrigated *in situ*. After suitable internal or external exposure to [^{3}H]ouabain, individual gill arches were excised for Na,K-ATPase assay, measurement of radiolabel binding, or quantitative high-resolution autoradiography. Internal exposure to 50 μM ouabain resulted in essentially complete enzyme inhibition, and binding paralleled the increases in enzyme activity at higher salinities; in contrast, external exposure gave minimal and erratic results consistent with leakage of external ouabain into interstitial fluid. [^{3}H]Ouabain autoradiographs demonstrated that, irrespective of exposure or salinity, most of the gill binding was associated with chloride cells. These cells increased in size and number with salinity and, at the subcellular level, the distribution pattern for bound ouabain was always identical to that for the amplified basal-lateral (tubular system) membrane. The combined physiologic-morphologic results constitute final direct proof that chloride cells are the primary site of gill Na,K-ATPase. More important, they provide convincing evidence for unexpected increases in basal-lateral enzyme at higher salinities and thus raise a fundamental objection to the long-postulated role of the Na pump in secretory NaCl transport.

Of various biochemical mechanisms thought to play important roles in salt-transporting epithelia, none has received more attention than the ouabain-sensitive, sodium- and potassium-dependent adenosine triphosphatase (Na,K-ATPase). The main role of this membrane-bound enzyme, associated with most animal cells, is thought to be the Na pump involved in maintenance of ion gradients

at the single cell level and in movement of salt across epithelial structures (1, 4). Na,K-ATPase activity is especially high in a number of osmoregulatory organs and appears to be correlated with the Na transport rate of the gland or tissue (42). One such organ, which has provided particularly suggestive data regarding Na,K-ATPase function, is the teleost gill (27, 28, 32). When certain bony fish (euryhaline teleosts) are adapted to a wide range of salinities, the gill responds with parallel changes in Na,K-ATPase activity and Na transport rate, e.g., activity and rate are low in fresh water (FW) and high in seawater (SW). Recently, adaptation to double-strength SW which is known to evoke still higher gill transport rates has been shown to induce still higher enzyme activity (20). In addition to functioning in osmoregulatory salt transport, the teleost gill is responsible for nitrogenous waste excretion and respiratory gas exchange. Of the several cell types present in gill epithelium, the most likely candidate for sodium (and chloride) transport is the chloride cell (27, 28). Chloride cells exhibit the two hallmarks of electrolyte-transporting epithelia, namely a rich population of mitochondria and a greatly amplified cell surface in the form of a basal-lateral tubular system. Moreover, chloride cell morphology in euryhaline teleosts also responds to changes in external salinity, e.g., the chloride cells are larger and/or more numerous in SW than in FW and the largest cells of all occur in fish adapted to environments more concentrated than SW (see companion paper [20] for discussion and literature). The question of the cellular location of gill Na,K-ATPase has been partly resolved by enzyme studies on isolated chloride cells (19, 41) and by preliminary, low-resolution, [^{3}H]ouabain autoradiographs of excised gills (28). Although these in vitro studies help to localize Na,K-ATPase to the chloride cell, they do not provide data at the subcellular level. Several cytochemical attempts at subcellular localization have shown ATPase reaction product associated with both the tubular system and the apical region of chloride cells (31, 44), but, given the ouabain-insensitivity of the reaction (Wachstein-Meisel Pb-capture), subcellular Na,K-ATPase "location remains a matter of dispute" (28).

In reviewing the technical difficulties of localizing ouabain-sensitive Na,K-ATPase, as distinct from other subcellular ATPase activities, Schwartz et al. (43) conclude that one promising method is the autoradiographic localization of specifically bound [^{3}H]ouabain. Using quantitative high-resolution autoradiography in conjunction with controlled [^{3}H]ouabain binding in perfused-irrigated gills, we have obtained convincing evidence that adaptive Na,K-ATPase is located not, as expected, on the apical membrane in chloride cells of SW fish (28), but on the amplified basal-lateral membrane or tubular system irrespective of environmental salinity. This paradoxical basal-lateral location in SW fish poses a major enigma concerning the role of the Na pump in salt secretion by gills and possibly other osmoregulatory epithelia.

MATERIALS AND METHODS

Animals and Media

Specimens of the euryhaline killifish *Fundulus heteroclitus* weighing 4–10 g were collected locally from May through November and stored in running SW tanks at 10–15°C. With Utility Seven Seas Mix (Utility Chemical Co., Patterson, N. J.) fish were adapted for 2–5 wk to 10%, 100%, or 200% artificial SW (Table I for Na concn) in aerated aquaria at 18–20°C. Fish destined for 10% and 100% SW were transferred directly to these environments; those destined for 200% SW were placed in 100% SW for 3 days, and then the salinity of their environment was increased in 21 equal steps by adding artificial sea salt at 12-h intervals. Food, in the form of chopped flounder, was provided weekly during storage and adaptation.

The gill vascular system was perfused with a modified Forster's (15) medium (NaCl, 135 mM; KCl, 2.5 mM; $CaCl_2$, 1.5 mM; $MgCl_2$, 1.0 mM; $NaHPO_4$, 0.5 mM; $NaHCO_3$, 7.5 mM) generally containing 1–2% bovine albumin (Fraction V, Sigma Chemical Co., St. Louis, Mo.), and the external surface was usually irrigated with 280 mM NaCl without albumin. In a few experiments, the irrigation medium also contained 25 mM KCl. Excised gill arches were incubated in either 280 mM NaCl or 100% artificial SW; free-swimming fish were exposed in the latter. Appropriate concentrations of radiolabeled ouabain and/or inulin (New England Nuclear, Boston, Mass.) were established in the above-mentioned media. Tritiated ouabain (supplied with about 10 Ci/mmol and diluted in unlabeled ouabain as necessary) was used at 1–5 μCi/ml for counting experiments and at 20 or 60 μCi/ml for autoradiography experiments. [*methoxy*-^{3}H]Inulin (731 mCi/g) or [*carboxyl*-^{14}C]inulin (3 mCi/g) was used at about 1 μCi/ml for counting experiments.

Perfused-Irrigated Gills

Fish were pithed, mounted ventral side up in a dissecting tray, and the opercula were partially cut and pinned back to expose the eight gill arches. The heart was exposed, and a polyethylene cannula was inserted through the ventricle and tied into the bulbus arteriosus.

The cannula was connected to an elevated 10-ml syringe which served as a reservoir for the perfusion medium. The liver was sliced to permit drainage of the perfusate. Oxygenated irrigation medium was dripped on the gills from a small piece of polyethylene tubing connected to a second reservoir.

The initial perfusion was done with heparinized medium without albumin, and the removal of blood cells (blanching) served as a first indication of the completeness of perfusion. Once the gills were blanched, time perfusion was begun by refilling the reservoir with medium containing labeled ouabain or inulin. The rate of perfusion was maintained at about 0.1 ml/min by regulating the height of the reservoir. After 45 min of uptake perfusion, the reservoir was refilled with ouabain- or inulin-free medium and washout perfusion was continued for another 25–30 min. During the entire 70–75 min no ouabain or inulin was present in the irrigation medium reservoir. At the end of the washout period, a tracer dye, Lissamine green, was added to the reservoir to check for leaks and completeness of perfusion. Gills were rejected if the perfusion rate could not be maintained or if the uptake of Lissamine was poor. At appropriate intervals during the course of uptake and washout, individual gill arches were excised for radiolabel counting, Na,K-ATPase assay, and/or autoradiography. The excision was performed with scissors and care was taken to crush the ventral stub so that leakage of vascular perfusate was minimized during continued perfusion-irrigation of the remaining arches. For the study of gill uptake from the external rather than the vascular side, labeled ouabain was introduced into the irrigation rather than the perfusion medium reservoir for the 45-min uptake period.

Incubated Arches and Free-Swimming Fish

Gill arches are excised immediately from pithed fish and stored for 5–10 min at 18–20°C in the appropriate medium, 280 mM NaCl or 100% SW. As expected, rapid clotting prevented gross leakage of blood, i.e. the gills remained red throughout storage and subsequent incubation. For incubation, individual gill arches weighing 10–15 mg were placed in capped 5-dram vials with 1.0 ml of oxygenated medium containing both [^{3}H]ouabain and [^{14}C]inulin. After moderate shaking at 18–20°C for 5 or 40 min, the arches were removed and processed for radiolabel counting. Free-swimming fish were placed in 35 ml of aerated 100% SW maintained at 18–20°C and containing both [^{3}H]ouabain and [^{14}C]inulin. After 45 min, fish were removed and pithed and blood was taken by cardiac puncture. The gill arches and kidney were excised and processed for radiolabel counting. The blood was centrifuged and a plasma sample obtained for counting.

Radiolabel Counting

Standard liquid scintillation counting procedures with internal quench correction were used to measure the ^{3}H and/or ^{14}C content of tissue and fluid samples. In preparation for counting, gill arches (bone plus filaments) and kidney tissue were blotted, weighed, and digested; measured volumes of corresponding fluids (e.g., perfusion medium, incubation medium, or blood plasma) were subjected to the same digestion procedure. Gill arches were rinsed before being blotted. The tissue content of labeled ouabain and/or inulin was generally expressed as an apparent distribution space based on the concentration in the medium to which the tissue has been exposed. Assuming unit tissue density, this space in percent tissue volume was calculated as dpm/gram tissue divided by dpm/0.01 ml medium. With perfused-irrigated gills, the ouabain remaining after washout was considered to be bound (see Results) and, since the corresponding autoradiographs never showed radioactivity over the bony arch itself, binding was expressed as micromoles ouabain per kilogram filament. On a wet weight basis the filaments comprised about 72% of the total gill arch, irrespective of the test environment to which fish were adapted (Table II).

Na,K-ATPase Assay

Excised gill arches were washed in ice-cold 5 mM EDTA, blotted, and the filaments were trimmed from the bony arch, weighed, and homogenized in the ratio of 20 mg of tissue to 1 ml of ice-cold 5 mM EDTA. Generally, filaments from at least two arches were pooled to provide sufficient homogenate for duplicate assays. The homogenate was filtered through nylon stocking, frozen by immersion of the vial in dry-ice-cooled absolute ethanol, and freeze-dried for 12–24 h at −20°C in the freeze-drier also used for autoradiography (below). These vials were stored at −10° to −20°C until the time of assay. Loss of Na,K-ATPase activity could not be detected even after 3 mo of storage.

All assays were performed in duplicate on freeze-dried homogenates reconstituted to 10 mg/ml in 5 mM EDTA just before use. The assay system was a modification of that used by Epstein et al. (9) and Ernst et al. (11). Homogenates were generally assayed at 37°C (Fig. 1, legend) for both total ATPase activity (Medium A) and ouabain-insensitive ATPase (Mg-ATPase) activity (Medium B). The concentration of the components in both Medium A and Medium B was adjusted to give the following final concentrations in a 1.5-ml reaction mixture: 6 mM ATP (disodium salt from Sigma Chemical Co.), 6 mM $MgCl_2$, 20 mM KCl, 100 mM NaCl, and 100 mM Tris-(HCl) buffer, pH 7.9. Medium B contained, in addition, 0.1 mM ouabain. Ouabain-sensitive ATPase (Na,K-ATPase) activity was determined by the difference between the activity measured with Medium A and the activity measured with Medium B.

Characterization studies on nonperfused gills from 100% SW-adapted fish showed that this reaction mixture was optimal for Na,K-ATPase activity and that the reaction rate was proportional to time and protein concentration. Also, 0.1 mM ouabain inhibited Na,K-ATP-

ase activity to the same extent as 1 mM ouabain or a potassium-free reaction mixture without ouabain (Fig. 1). Protein was determined by the technique of Lowry et al. (24) with bovine albumin serving as the standard. For 10%, 100%, and 200% SW-adapted fish, the milligrams protein/gram filament averaged 43 ± 2 SE (five fish), 43 ± 8 (six), and 42 ± 7 (six), respectively.

Normal Morphology and Ultrastructure

Nonperfused gills from five specimens adapted to each environment were used exclusively for morphological study. Individual arches were fixed for 3 h at room temperature with 6% glutaraldehyde in 0.2 M cacodylate buffer (17) at pH 7.4. After fixation, they were washed in 0.2 M cacodylate buffer at the same pH, and postfixed for 90 min at 0–5°C in 1% osmium tetroxide prepared in the same buffer. After three quick rinses in tap water at 0–5°C, the fixed tissue was rapidly dehydrated through increasing concentrations of ethanol and embedded in Epon (25). In addition, nonperfused gills from several 100% SW-adapted fish were prepared as above, except that the initial fixative was a mixture of 1% acrolein, 1% formaldehyde, and 1% glutaraldehyde (39) in 0.2 M phosphate buffer at pH 7.4, and the subsequent wash was with this same buffer.

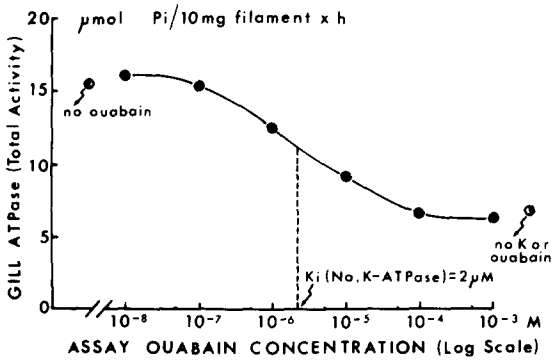

FIGURE 1 Ouabain inhibition of Na,K-ATPase in homogenate of nonperfused gill filaments from a 100% SW-adapted killifish. This in vitro dose-response curve was generated using the standard 37°C assay procedure (text) and varying the ouabain concentration in the reaction mixture. Each point represents the mean for duplicate assays. Comparison points represent no ouabain or no ouabain or potassium; sodium was present in all assays. Results are expressed as total ATP-splitting activity, i.e. the summed action of Mg-ATPase (ouabain insensitive) and Na,K-ATPase (ouabain sensitive). The half-inhibition concentration of ouabain (Ki) was obtained by interpolation. A nearly identical Ki value was obtained from a second dose-response curve (not shown) generated with pooled gill homogenate from several 100% SW fish and with the assay temperature lowered to 20°C, i.e. the temperature of the perfusion-irrigation experiments.

Sections for light microscopy (0.8–1.2 μm) were cut with glass knives and stained with methylene blue and Azure II (38). Thin sections (500–800 Å) were cut with a diamond knife, stained for 5 min with 2% aqueous uranyl acetate adjusted to pH 5 with 1 N NaOH, washed in distilled water, and counterstained for 5 min with lead citrate (37). The sections were examined with a Hitachi HU-11C electron microscope operated at 75 kV.

Autoradiography

[^{3}H]Ouabain autoradiographs were prepared from freeze-dried plastic-embedded sections of gill arches according to the method originally described by Stirling and Kinter (48). After perfusion or irrigation exposure to [^{3}H]ouabain, individual arches were excised and rapidly frozen in liquid propane at about −185°C. Frozen gill arches were stored for up to several weeks in liquid nitrogen and then freeze-dried in batches, using a Virtis 10-010-C-TDP-CA cascade refrigerated freeze-drier designed for temperature-controlled tissue drying (The Virtis Co., Gardiner, N. Y.). With a vacuum of about 1 μm and the condenser at −85°C, the tissue drying schedule was as follows: 3 days at −55°C, 12 h each at −40° and −20°C, and 30 min each at 0° and about 25°C. The last temperature was always several degrees above room temperature to prevent condensate from rewetting the tissue upon removal from the drying chamber. The dried gill arches were fixed overnight in osmium tetroxide vapor, cut into small pieces each with 5–10 filaments, and embedded in a silicone-impregnated epoxy resin, Spurr Low-Viscosity (Polysciences, Inc., Warrington, Pa.). Before polymerization, the pieces were oriented so that the individual filaments would be sectioned transversely; after polymerization, the tips of the filaments were trimmed away, since the distal third of a filament generally contains few chloride cells. Light-microscope sections (0.8–1.2 μm) were cut with glass knives and generally collected over water, dried onto microscope slides, and dipped in Eastman Kodak NTB-2 emulsion diluted with an equal volume of distilled water. After drying, the thickness of the emulsion coat was about 2 μm. Occasionally, special modifications (26) were employed to prevent tissue sections from coming into contact with water or liquid emulsion. After a suitable period of autoradiographic exposure, usually 10–50 days, slides were developed in Kodak D19, fixed in Kodak rapid fixer, and lightly stained with methylene blue and Azure II. The final autoradiographs were examined and photographed with a light microscope equipped with Zeiss phase-contrast optics. Evaluation for technical artifacts revealed neither gross leaching of [^{3}H]ouabain into the embedding plastic or the emulsion coat nor any tissue-induced chemography, positive (chemical fogging) or negative (latent-image fading). Moreover, reciprocity between grain density and exposure time was observed over both chloride cells and [^{3}H]ouabain standards (below), confirming the absence of latent-image fading and indicating that the emulsion was not saturated at densi-

ties employed for grain counting (<500 grains/1,000 μm^2).

For quantitative grain density analysis of chloride cells, emulsion grains were counted under phase optics so that various cell types and regions could be accurately identified. An ocular grid was used to quantitate the areas over which grains were counted and, at the magnification employed, grid squares were 3.9 μm on a side. Grains were counted over the non-nuclear portion of all chloride cells associated with a given filament (transverse section) and over adjacent plastic alone (background). Each cell count for a given filament consisted of at least 100 grains and each experimental fish (Table II) was represented by six filaments, three from each of two tissue sections which were cut from different pieces of gill arch, dried onto different slides, and often exposed for different times. The variability (±SD in percent of mean) of the chloride cell, minus background, density (grains/1,000 μm^2 × days exposure) for the six individual filaments from each fish was consistently within ±20%, which is somewhat less than the variability of absolute density values originally observed with sections of ^{3}H-standards on different slides (48).

Because all grid areas completely filled by non-nuclear portions of chloride cells were counted for each filament sampled, we used the total number of grid areas counted to estimate the relative chloride cell "volume" at each test environment (Table II).

For converting grain density to ouabain content, standard solutions of [^{3}H]ouabain in 10% albumin were rapidly frozen and processed in the same way as gill tissue. The plot of grain density for [^{3}H]ouabain standards (grains/1,000 μm^2 × μM ouabain) against exposure time of autoradiographs (days) gave a straight line which passed through the origin, demonstrating reciprocity. Assuming unit specific gravity for chloride cells, the slope of this line was used to derive ouabain content in micromoles/kilogram cell.

RESULTS

Characterization of Perfused-Irrigated Gills Exposed to Ouabain from the Vascular Side

For autoradiographic localization of bound [^{3}H]ouabain to be meaningful, it was necessary to establish that this inhibitor is bound specifically to the gill Na,K-ATPase. During exposure to ouabain via the vascular perfusion medium, gills must contain both bound and free molecules. Moreover, since ouabain does not generally enter the intracellular space, we anticipated that the free or unbound molecules would be distributed only in the extracellular space, i.e. interstitial fluid and vascular perfusion medium. Any free molecules escaping from the gill surface would be washed away by the external irrigation medium. In early experiments, individual gill arches were excised at frequent time intervals to evaluate total uptake and subsequent washout during perfusion with 50 μM ouabain and ouabain-free media, respectively. Each excised arch (filaments plus bone) was analyzed for radiolabeled ouabain content. As shown in Fig. 2, 45 min of ouabain perfusion was ample to ensure a steady state with regard to total uptake (expressed as the apparent distribution volume or space) in fish adapted to each of the three test environments. Note that total ouabain uptake increased with the salinity of the environment, suggesting increased binding. In all fish subsequent perfusion with ouabain-free medium for 25 min resulted in a rapid washout of some molecules and a new steady-state distribution space (Fig. 2). This remaining distribution space was taken to represent bound ouabain (below) and the decrease in steady-state distribution was termed "washout space" (illustrated for 200% SW data in Fig. 2). Generally, washout space was computed on the basis of the difference between the ouabain content of an arch excised after 45 min of uptake and that of another after 25 min of washout. In later perfusion experiments, other arches were excised at these times for ATPase assay and autoradiography.

All washout space data for gill experiments with 50 μM ouabain in the vascular perfusion medium are summarized in Table I. Irrespective of the environment, the mean washout spaces are close enough to a typical whole fish extracellular space of 15% (18) to permit the conclusion that vascular washout removed primarily the free ouabain distributed in extracellular fluids during uptake. This conclusion is supported by results from additional perfusion-irrigation experiments with radiolabeled inulin, a classical unbound extracellular marker, present in the vascular medium. Only 10 min of uptake perfusion appeared sufficient to give steady-state inulin distribution spaces which, in percent gill arch volume, averaged 15.1 ± 1.8 SE for nine fish representing all three test environments. An extracellular space of 15% is reasonable, considering that about 25% of the gill arch consists of bone on a wet weight basis (Table II). Furthermore, washout with inulin-free medium proceeded rapidly enough to indicate reasonably complete perfusion of the gill vascular system, i.e., inulin space values in percent had dropped to 6.7 ± 0.8 SE (seven), 4.9 ± 0.9 (six), and 3.5 ± 1.0 (three) by 10, 20, and 30 min, respectively. On

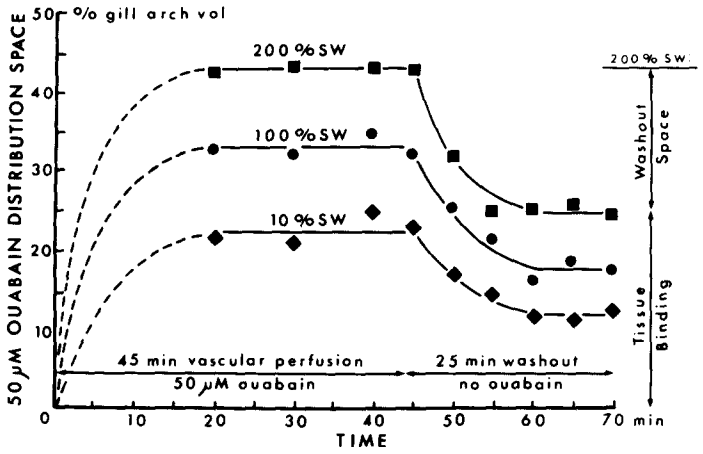

FIGURE 2 Time course of [^{3}H]ouabain uptake and washout in perfused-irrigated gills exposed from the vascular side. In all experiments, the vascular perfusion medium consisted of Forster's saline with 1–2% albumin and, from 0 to 45 min, 50 μM ouabain (1–5 μCi ^{3}H label/ml); the external irrigation medium consisted of 280 mM NaCl alone (see Materials and Methods). Data for each test environment (i.e. 10%, 100%, and 200% seawater) are from four adapted killifish, and individual points represent mean values for two to four gill arches, each excised from a different fish. For purposes of presentation, these data are expressed as the "50 μM ouabain distribution space," i.e. the percentage of the whole gill volume in which the measured ouabain content could be distributed at this concentration (see Materials and Methods). Actually, since some or all of the contained ouabain molecules are bound, the calculated distribution space must be considered an apparent rather than a real value.

TABLE I

*[^{3}H]Ouabain Uptake from Vascular Perfusion Medium and Na,K-ATPase Activity in Gills of Killifish Adapted to Sea Water (SW) Mixtures**

Na concn‡		Gill ouabain with 50 μM perfusion		Gill Na,K-ATPase		
					Perfusion	
Environment	Plasma	Washout space§	Tissue binding	Nonperfused gill	Control	50 μM Ouabain
meq/liter		*% gill arch vol*	*μmol/kg filament*	*μmol P_i/10 mg filament × h*‖		
780 (200% SW)	207 ± 6 (6)	16.4 ± 2.2 (7)	16.7 ± 1.0 (7)	12.1 ± 0.9 (6)	13.3 (2)	2.1 ± 0.2 (4)
390 (100% SW)	175 ± 5 (6)	13.0 ± 1.5 (8)	11.1 ± 1.0 (8)	5.7 ± 0.7 (6)	7.3 (2)	0.8 (2)
40 (10% SW)	158 ± 4 (6)	10.7 ± 2.2 (5)	6.9 ± 0.6 (5)	3.5 ± 0.3 (5)	3.7 (2)	1.0 (2)

* Values generally expressed as mean ± SE *(n)*, where *n* is the number of fish. Plasma Na, non-perfused gill ATPase, and tissue binding of ouabain in 200% and 10% SW fish differed significantly from 100% SW values ($P < 0.01$, except 0.025 for binding in 10% SW).

‡ Measured by flame photometry.

§ See Fig. 2 and text for definition and calculation.

‖ Multiply by 2.3 to convert to micromoles P_i/milligram protein × hours (see Materials and Methods).

the other hand, the 20- and 30-min values are larger than expected for washout of a single diffusional compartment, suggesting some limitation of perfusion. Gills with grossly incomplete vascular perfusion were excluded on the basis of low flow rates and/or visual checks, i.e. initial blanching

TABLE II

*Binding in Killifish Gills Perfused with 50 μM [^{3}H]Ouabain**

Fish adapted for 2–5 wk	Gill filaments‡		Chloride cells§	
	Wet weight	Ouabain binding	Ouabain binding	Estimated volume (relative)
	% arch	*μmol/kg*		
200% SW	75 ± 2 (4)	16.7 ± 1.0 (7)	300 ± 10 (4)	1.8 ± 0.1 (4)
100% SW	71 ± 1 (4)	11.1 ± 1.0 (8)	240 ± 20‖ (4)	1.0 ± 0.2 (4)
10% SW	71 ± 1 (4)	6.9 ± 0.6 (5)	250 (2)	0.8 (2)

* Values generally expressed as mean ± SE *(n)*, where *n* is number of fish. Chloride cell binding and volume in 200% SW fish differed significantly from 100% SW values ($P < 0.01$ for volume). Arch weights did not differ significantly.

‡ Based on liquid scintillation counting.

§ Based on autoradiographic grain density measurements; values are for the non-nuclear portion of these cells (see text for subcellular localization of bound ouabain).

‖ Total ouabain content for these four fish average 270 ± 15 μmol/kg chloride cell before 25 min washout ($P > 0.05$ compared to bound ouabain remaining after washout).

with washout of blood and terminal staining with Lissamine green (see Materials and Methods). However, abnormal vascular resistance and shunt diversion of flow are known to pose problems in perfused gills (3, 21, 36), and examination of present ouabain autoradiographs has occasionally revealed red cell-clogged vessels near regions of reduced radioactivity (see Materials and Methods). Thus, local regions of limited perfusion probably existed in all of our perfused-irrigated gill experiments. This question will be considered further with regard to Na,K-ATPase inhibition after ouabain perfusion.

Since further decrease in the ouabain content of perfused gills could not be detected after 25 min of washout (Fig. 2), all remaining ouabain was judged to be bound to gill tissue. Moreover, as shown by autoradiography, this bound ouabain was located primarily in the filaments rather than the remaining bony part of the gill arch. Table I summarizes all tissue binding data in micromoles ouabain/kilogram filament resulting from vascular exposure to 50 μM ouabain. In contrast to washout space, tissue binding increased dramatically with the salinity of the external environment to which the fish has been adapted. Moreover, results from experiments with ouabain concentrations both lower and higher than 50 μM (example below) indicated that the values in Table I represent near maximal or saturation binding for each environment, i.e. that most of the potential binding sites were already filled by exposure to the free ouabain concentration established in extracellular fluids during perfusion with 50 μM ouabain. For example, with 100 μM ouabain in the vascular medium the binding in micromoles/kilogram filament averaged 11.4 ± 1.2 SE for four fish adapted to 100% SW. Likewise, for several fish adapted to 10% and 200% SW, the binding values were only slightly above those in Table I. Also, as expected, the 100 μM washout space in percent gill arch volume was essentially unchanged, averaging 16.7 ± 1.1 SE for eight fish representing all three environments. Finally, it should be noted that the limited increases in plasma sodium concentration observed after 2–5 wk of adaptation to test environments ranging from 10% to 200% SW (Table I) agree with the general pattern for euryhaline teleosts (14, 18, 46) and indicate successful adaptation of the present killifish, i.e. the salt transport mechanism of the gill and other osmoregulatory organs had adjusted to meet the particular osmotic stress of each of the three test environments.

Assay of the Na,K-ATPase activity provided an additional means of characterizing the ouabain binding in perfused-irrigated gills. As shown in Table I, the level of Na,K-ATPase activity in filaments from nonperfused, nonirrigated gills, i.e. from freshly sacrificed fish, increased with the

salinity of the external environment to which the fish had been adapted. Increased enzyme activity is in accord with numerous observations in euryhaline species adapted to salinities between FW and 100% SW, and the still higher level at 200% SW agrees with the only other report at this salinity (see the introductory paragraphs). In fact, our actual Na,K-ATPase values at 10% and 100% SW (Table I) are similar to the FW and SW values published by Epstein et al. (9) for whole homogenates of fresh *F. heteroclitus* gill (see Materials and Methods for conversion of ATPase activity per 10 mg filament to per milligram protein). Equally important, perfusion-irrigation per se did not alter the activity of this enzyme, i.e. control levels after 70 min with ouabain-free vascular and external media did not differ grossly from fresh nonperfused levels (Table I). On the other hand, perfusion with 50 μM ouabain in the vascular medium for 45 min followed by washout for 25 min did decrease the enzyme activity at each environment by about 80%. This finding also agrees with earlier observations that ouabain is an effective Na, K-ATPase inhibitor from the vascular side in fish gills (45, 49). The question next arises as to whether all of the gill Na,K-ATPase is inhibitable from the vascular side. As calculated from the ouabain dose-response curve generated under in vitro assay conditions with a gill filament homogenate (Fig. 1), inhibition should have been 92% complete at 50 μM if all the enzyme were exposed. Thus, only a small discrepancy exists between in vitro and in situ inhibition, which probably reflects local regions of limited vascular perfusion (above) where the enzyme was not exposed to the full ouabain concentration. If so, all of the gill Na,K-ATPase may be inhibitable from the vascular side (Discussion). At any rate, we can conclude from the high degree of *in situ* inhibition from the vascular side (about 80% inhibition) that the ouabain-enzyme complex represents very stable binding, since the bond survived the diluting effects of both the 25-min washout and the assay procedure. For example, if all 11.1 μmol of bound ouabain/kg filament (100% SW fish) had come off during dilution to 0.67 mg filament/ml Na,K-ATPase assay medium, the resulting ouabain concentration of about 10^{-8} M would have been too low to produce any enzyme inhibition (Fig. 1).

Since *in situ* vascular exposure of the gill to 50 μM ouabain results in nearly complete inhibition of Na, K-ATPase, the observation that tissue ouabain binding and Na,K-ATPase activity increase in a parallel fashion with increase in external salinity (Table I) provides convincing evidence for specific binding of ouabain to this enzyme with negligible nonspecific binding to other potential tissue sites. Comparing, for example, 10% SW and 100% SW gills, both ouabain binding and enzyme activity nearly doubled. Moreover, our evidence for specific ouabain binding *in situ* is corroborated by the recent in vitro work of Sargent and Thomson (40) with enriched enzyme fractions of gill homogenate from FW- and SW-adapted eels. Under conditions which precluded the problem of incomplete vascular perfusion and optimized the exposure of enzyme sites through tissue disruption and fractionation, they obtained an exact quantitative correspondence between ouabain binding and Na,K-ATPase activity. Also, they showed that the FW and SW enzymes were indistinguishable on the basis of several properties, including displacement of ouabain binding by potassium. Thus, as cell integrity is destroyed by in vitro homogenization, *in situ* perfusion which only slightly compromises ouabain exposure becomes the method of choice for autoradiographic localization at the cellular level. The well-known cardiovascular effects of ouabain preclude in vivo study with high ouabain concentrations in the blood.

Autoradiography of Perfused-Irrigated Gills Exposed to Ouabain from the Vascular Side

Having established that [^{3}H]ouabain tags only gill Na,K-ATPase, i.e. binding *in situ* is stable and specific, we proceeded to the primary objective, autoradiographic localization of this enzyme in gill filaments. The major histological features of the tissue are shown in Fig. 3. The respiratory leaflets, which project from the sides of the filament, consist of pillar cells and respiratory epithelial cells. The filament itself is supported by a central cartilaginous spine embedded in the connective tissue core; afferent and efferent branchial arterioles are located at opposite ends. Of special interest for the present study is the distribution of the various cell types in the epithelium overlying the central core, i.e. between the respiratory leaflets. The pavement cells form the main surface covering but are absent where mucous and chloride cells are directly exposed to the external environment. Between the pavement cells and the basal lamina,

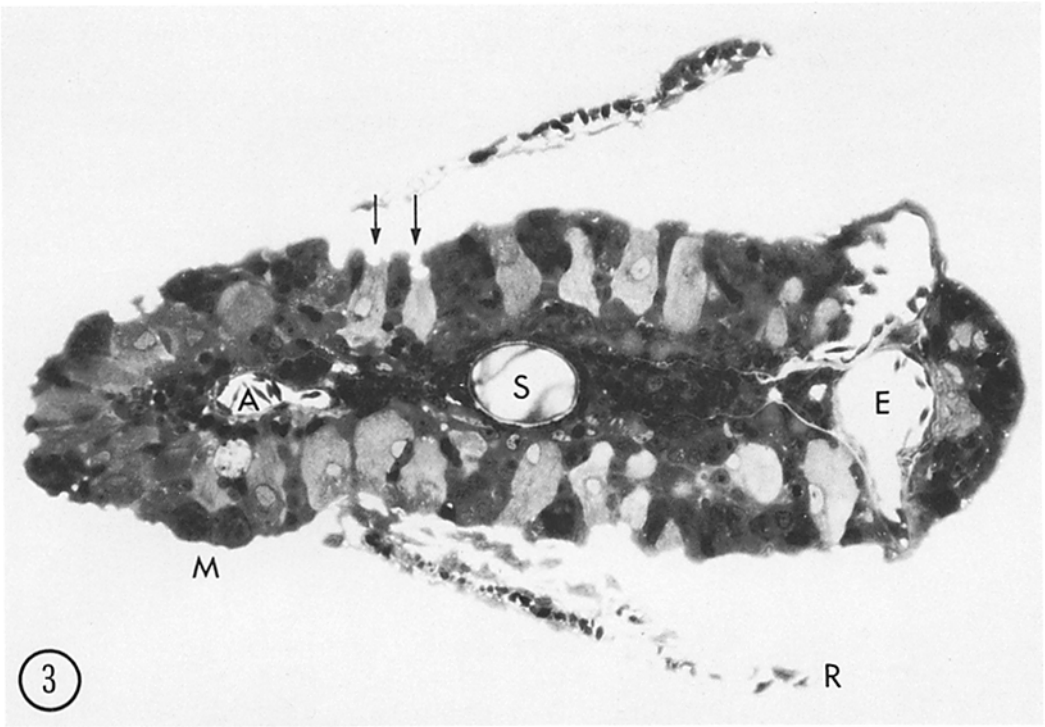

FIGURE 3 Normal morphology of a single nonperfused gill filament from a 100% SW-adapted *F. heteroclitus*. Cut at a level between respiratory leaflets (see text), this transverse section shows a minimal amount of respiratory tissue *(R)* and a maximal amount of other tissue, including darkly stained mucous cells *(M)* and lightly stained chloride cells (arrows). The central connective tissue core includes a supporting cartilaginous spine *(S)*, and, at opposite ends, a smaller afferent *(A)* and a larger efferent arteriole *(E)* both containing some nucleated red blood cells. Among the cell types in the epithelium overlying this core, the chloride cells are especially prominent because of their large, columnar shape, granular cytoplasm and apical crypts (arrows). Processed for normal morphology (aldehyde mixture fixation), this heavily stained, 1-μm plastic section was photographed with bright-field optics. × 400.

mucous and chloride cells are embedded in stratified layers of supporting epithelial cells. The columnar-shaped chloride cells are clearly the largest in the gill epithelium, typical dimensions being 8 μm in width and 20 μm in length. The nucleus is basal and the cytoplasm is dominated by mitochondria. Favorable sections show that the apical surfaces of these cells are invaginated to form a pit or crypt that is directly exposed to the external environment. As shown in Fig. 3, most chloride cells are located at the afferent blood vessel end of the filament. Our observations conform to the classical description given by Copeland (6) for SW-adapted specimens of this species.

Rapid-freeze, freeze-dry, plastic-section autoradiography provides a direct means for visualizing the tissue distribution of [^{3}H]ouabain at the light microscope level. The autoradiographs in Figs. 4 and 5 show the chloride cell-rich ends of individual filaments representative of gills from 200% SW and 10% SW fish after vascular exposure to ouabain. Two facts are immediately clear: the majority of the autoradiographic grains were always associated with the chloride cells irrespective of environment, and these cells were larger and more numerous in fish adapted to higher salinity environments. Other cell types, e.g., mucous cells and respiratory epithelium (not shown), and other tissue elements, e.g., cartilaginous spine and bony arch (not shown), never exhibited the dense pattern of grains seen over chloride cells. This dense grain pattern, reflecting extensive binding of radiolabeled ouabain molecules by chloride cells, was observed consistently after vascular exposure both to 3 μM (Figs. 4, 5) and to 50 μM (Fig. 9) high specific activity, 1–8 Ci/mmol, [^{3}H]ouabain,


A
S
4

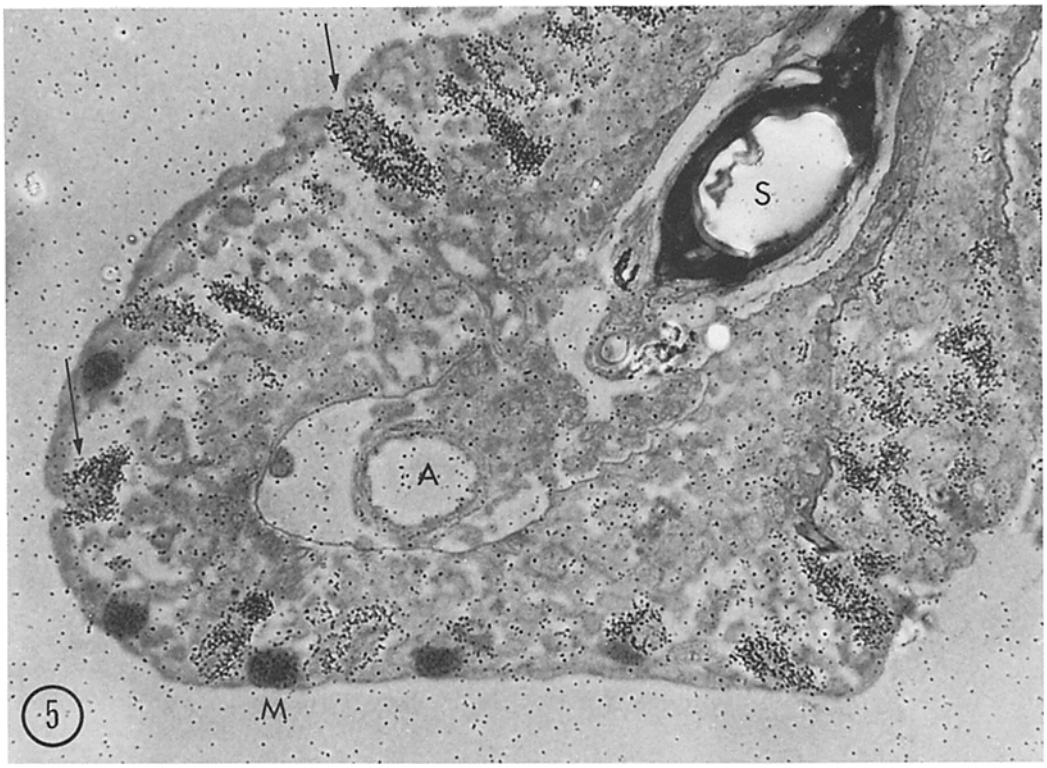
S
A
M
5

but was almost undetectable after exposure to 1,000 μM low specific activity, 0.02 Ci/mmol, [^{3}H]ouabain (not shown). This attenuation of the grain pattern indicates competition of unlabeled ouabain molecules for a finite number of chloride cell binding sites. Moreover, the ouabain affinity of these sites appears to be correct for binding to Na,K-ATPase, i.e. saturation above 50 μM ouabain (Fig. 1). The question of subcellular localization of the binding sites will be considered in the next section.

Autoradiographic grain density counting provides a direct quantitative measure of maximal chloride cell binding after vascular exposure to a saturation level of ouabain, e.g., 50 μM. As shown in Table II, the amount of ouabain bound per unit weight or volume of chloride cell (nonnuclear portion, below) was almost the same for all three test environments. On the other hand, the relative cell volume, estimated in the course of grain counting (see Materials and Methods), did increase progressively with salinity. As reported by many investigators (see introductory paragraphs) and as seen in Figs. 4 and 5, this increase reflects both size and number of individual chloride cells. Since overall chloride cell binding is the product of unit binding and cell volume, there was a 2.7-fold increase from 10% SW fish to 200% SW fish which would easily account for the directly measured 2.4-fold increase in whole gill filament binding (Table II). Also, consistent with chloride cells' possessing most of the gill ouabain, unit chloride cell binding in micromoles/ kilogram was many times (36–18) greater than whole gill filament binding in micromoles/kilogram (Table II). In fact, the calculated percentage of the filaments which would have to be composed of chloride cells in order to account for all filament binding increased from 3% of the filament at the lowest to 6% at the highest salinity environment. This increase agrees well with our independently estimated increase in relative chloride cell volume (Table II). Also, Sargent and Thomson (40) have reported 5–10% chloride cells in gills from SW eels. In conclusion, autoradiography at the cellular level clearly indicates that after vascular exposure most of the gill ouabain is bound by chloride cells.

Subcellular Localization of Bound Ouabain

At low magnification (Figs. 4 and 5), the autoradiographic grain pattern appears to be uniformly distributed over the "cytoplasm," i.e. the nonnuclear portion of the chloride cells, thus suggesting an intracellular locus for binding sites. However, we know of no precedent for rapid intracellular penetration of ouabain and it is well known that the teleost chloride cell possesses an extensive, anastomosing tubular system which is in direct communication with interstitial fluid. In effect, the tubular system represents an enormous amplification of the plasma membrane at the basal and lateral cell surface (see introductory paragraphs). The tubules extensively invade the cytoplasm and are poorly represented only in the supranuclear Golgi regions and a narrow zone adjacent to the apical crypt (Fig. 6). They are completely absent from the cell nucleus. This tubular system distribution was similar in chloride cells from all fish regardless of test environment. Ultrastructural examination of the tubules, however, revealed that there were slightly more tubules per unit volume of cytoplasm in chloride cells from fish adapted to 200% SW (not shown). This observation is in general agreement with the findings

FIGURE 4 Autoradiograph from 200% SW fish gill after 45 min of vascular perfusion with 3 μM [^{3}H]ouabain (20 μCi/ml) and 25 min of washout. The underlying tissue section is oriented as in Fig. 3 and shows the chloride cell-rich end of a filament with the afferent arteriole *(A)*, partly collapsed, and part of the cartilaginous spine *(S)*. The developed silver grains in the autoradiographic emulsion appears as fine black dots, and the highest density is associated with the nonnuclear portion of chloride cells (arrows indicate cells with nuclei showing). 1 μm section of freeze-dried, plastic-embedded tissue coated with a 2-μm layer of emulsion, exposed for 48 days for qualitative visual evaluation (long exposure gave high background density), and photographed with phase-contrast optics. × 600.

FIGURE 5 Autoradiograph from 10% SW fish gill after 45 min of vascular perfusion with 3 μM [^{3}H]ouabain (20 μCi/ml) and 25 min of washout. Details as given for companion autoradiograph (Fig. 4), except that arrows indicate chloride cells with crypts showing and several mucous cells *(M)* are present. × 600.

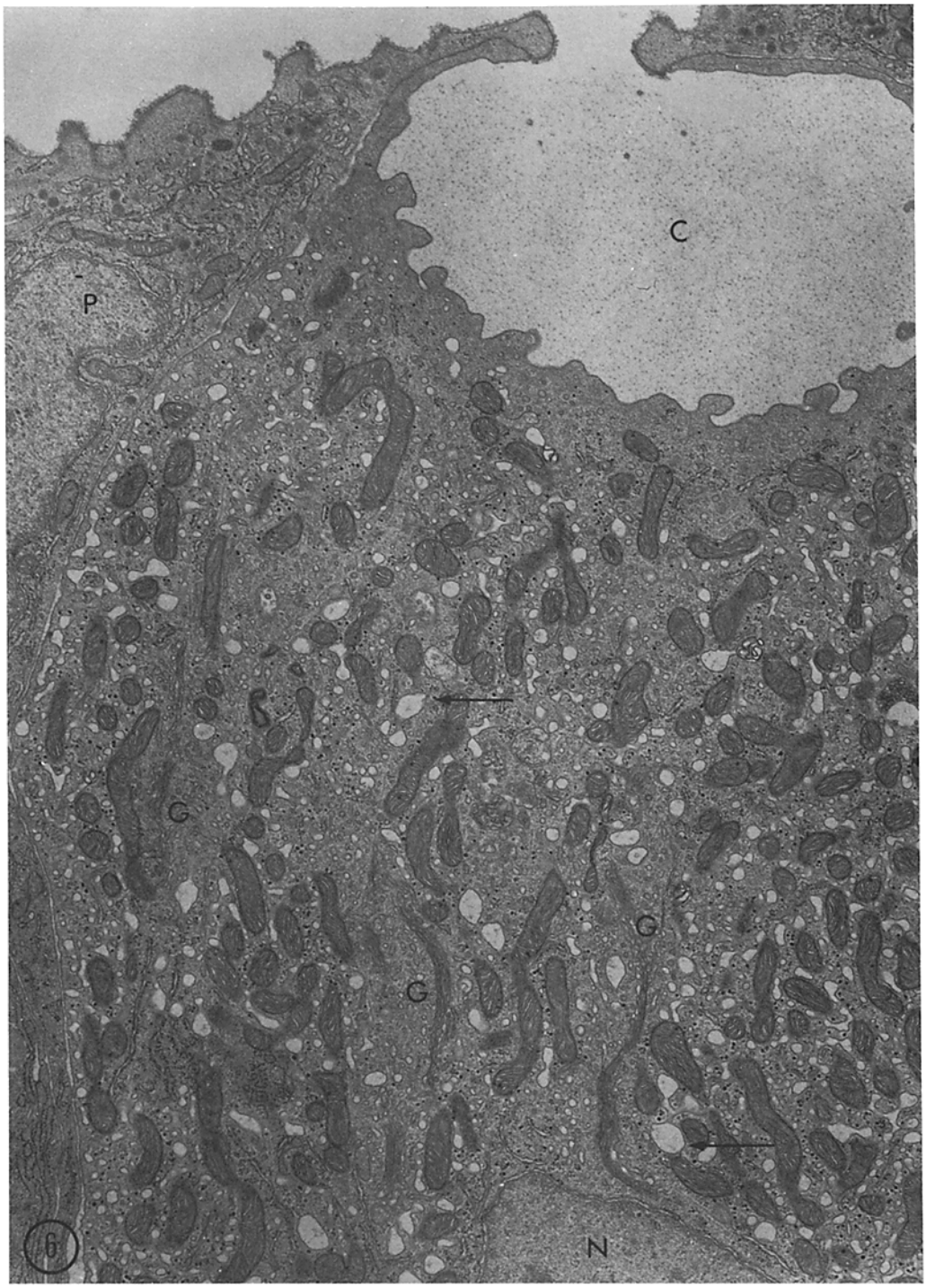

FIGURE 6 Electron micrograph of nonperfused gill filament epithelium from a 100% SW-adapted *F. heteroclitus*. This low magnification view shows part of a pavement cell *(P)* and most of the apical half of a chloride cell with a prominent crypt *(C)*. Above the nucleus *(N)* of this cell are several regions of supranuclear Golgi complex *(G)*. Except for a narrow zone adjacent to the apical crypt, the cell cytoplasm, both apical and basal (not shown), is heavily interspersed with numerous mitochondria (darkly stained) and the extensive tubular system (electron translucent). Some of the individual tubules are rather dilated (arrows). Thus, the tubular system and the mitochondria exhibit an almost identical distribution pattern within the cell, i.e. absent from nucleus, Golgi, and crypt zone and uniform throughout the remainder of the cell. Chloride cells from 10% SW and 200% SW fish gills exhibited an almost identical ultrastructure, except that there were slightly more tubular profiles in 200% SW fish (not shown). Processed for normal ultrastructure (glutaraldehyde fixation). × 25,200.

in *Cyprinodon variegatus* (20), i.e. the same tubular density in 50% and 100% SW fish and a large increase in 200% SW fish, which was associated with an almost fourfold increase in gill Na,K-ATPase.

When examined at higher magnification light microscope level autoradiographs revealed that the grain density pattern in non-nuclear regions of chloride cells was not exactly uniform but, at all environments, followed closely the distribution pattern of the tubular system (Fig. 7). Areas of lowest grain density were the Golgi region and the region adjacent to the apical crypt, precisely the regions where the tubules are less well represented. If the grain distribution pattern indeed reflects tubular localization, then we would expect to find a slightly higher amount of ouabain bound per unit weight or volume of chloride cell in 200% SW fish, as, in fact, we did (Table II). Autoradiographic grain counting was also used in an attempt to demonstrate "washout" of unbound ouabain from the lumen of the tubular system (in effect, part of the interstitial fluid compartment) by comparing chloride cells in gill arches frozen immediately after [^{3}H]ouabain perfusion with chloride cells in those frozen after the usual 25 min of additional washout. For the 100% SW-adapted fish in Table II (see footnote to Table II) the total ouabain content of the cells before washout was higher by about 12%. Although this difference is not statistically significant (variability of grain counting was a limiting factor), it is of inter-

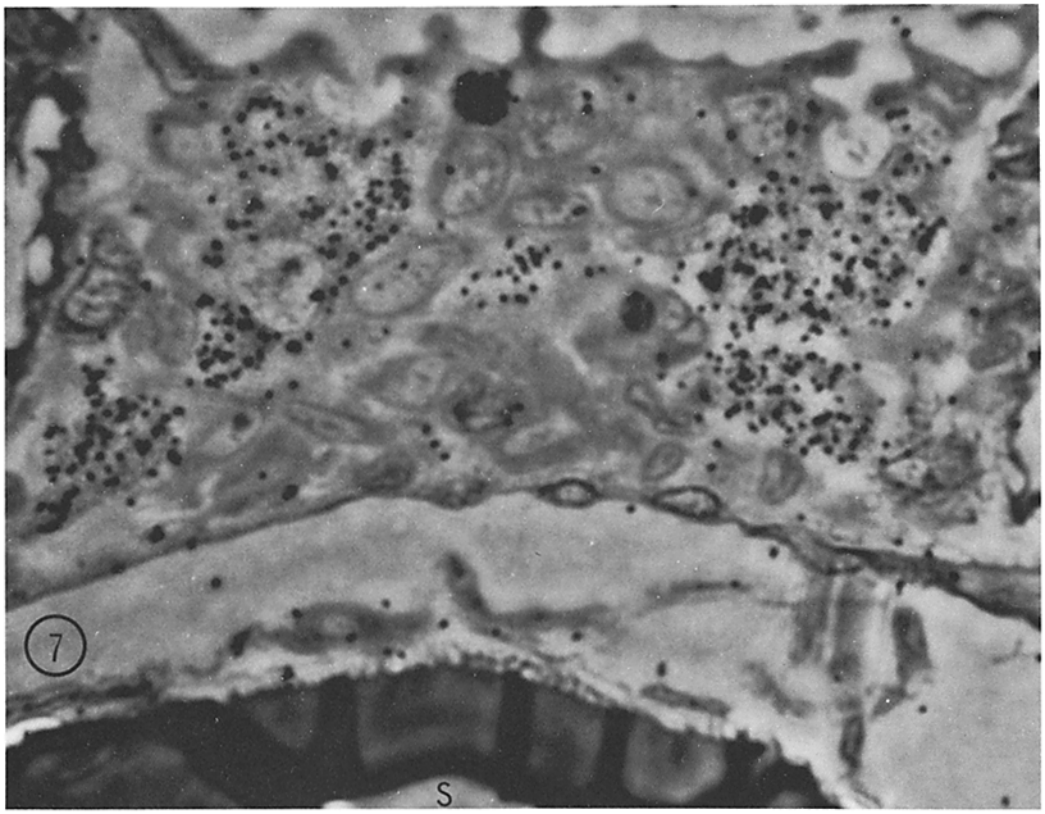

FIGURE 7 Autoradiograph from 100% fish gill after 45 min of vascular perfusion with 50 μM [^{3}H]ouabain (60 μCi/ml) and 25 min of washout. The underlying tissue section shows two large chloride cells (with prominent apical crypts) in the epithelium above the filament cartilaginous spine *(S)*. The developed silver grains in the autoradiograph emulsion appear as black dots and are distributed rather uniformly over the cytoplasm except for the nucleus (chloride cell at left), isolated areas in the supranuclear region, and a narrow zone adjacent to the apical crypt. 1 μm section of freeze-dried, plastic-embedded tissue coated with a 2-μm layer of emulsion, exposed for 30 days, and photographed with phase-contrast optics. × 2,050.

est that the apparent unbound ouabain could have been contained at 50 μM in a volume of interstitial fluid equal to 60% of chloride cell volume. At the whole tissue level, visual comparison of the same autoradiographs always showed more ouabain in connective tissue and blood vessel regions before washout. In conclusion, autoradiography at the subcellular level strongly suggests that after vascular exposure most of the chloride cell ouabain is bound to the tubular system membrane. Remaining, however, is the important question of whether additional ouabain binding can be demonstrated at membrane sites not facing vascular or interstitial fluid, e.g., at the apical crypt membrane of the chloride cell.

Perfused-Irrigated Gills Exposed to Ouabain from the External Irrigation Side

The perfused-irrigated gill system was also used to explore the possibility of externally located Na,K-ATPase. After exposure of gills to 50 μM ouabain in the external irrigation medium for 45 min, followed by 25 min of wash, both Na,K-ATPase inhibition and ouabain binding were minimal (Table III). Also, there was no distinct correlation between the small binding values and the increased enzyme levels found with adaptation to higher salinity environments. These results contrast markedly from those after vascular exposure, i.e. with 50 μM ouabain in the perfusion medium (Table I). In fact, the existence of a finite washout space after irrigation exposure (Table III) suggests that small amounts of ouabain may have simply leaked across the gill epithelium into the interstitial fluid. If the resulting ouabain concentrations at the interstitial fluid (tubular system) side of the chloride cells were variable and low, only a small percentage of the binding sites would be filled and there would be no distinct correlation with the total enzyme level. Actually, both washout space and tissue binding were variable and roughly only 10% of the corresponding values after vascular exposure (Table III). Also, the fact that tissue binding was unaffected by 25 mM potassium in the irrigation medium (Table III) argues against external sites since high potassium concentrations generally decrease the binding of ouabain (16, 43).

Further evidence for leakage of ouabain from irrigation medium to interstitial fluid was provided by autoradiographs. The low magnification view in Fig. 8 shows the extreme variability of grain distribution found even in adjacent gill filaments after irrigation exposure and washout. Numbers of grains in individual filaments ranged from almost none to densities actually approaching those seen with vascular exposure. In those filaments with grains, the majority were associated with chloride cells (Fig. 8). In autoradiographs prepared before the final washout step (not shown) filaments with heavily grained chloride cells also exhibited finite numbers of grains in extracellular spaces, e.g., blood vessel lumens. These results are consistent with localized leakage through the epithelium of

TABLE III

*[^{3}H]Ouabain Uptake from Irrigation Medium and Na,K-ATPase Activity in Gills of Killifish Adapted to Seawater (SW) Mixtures**

	Gill Na,K-ATPase		Gill [^{3}H]ouabain		
				Tissue binding	
Environment	Nonperfused gill	Irrigated 50 μM ouabain, no K	50 μM washout space‡	no K	25 mM K
	μmol P_i/10 mg filament × h		*% arch vol*	*μmol/kg filament*	
200% SW	12.1 ± 0.9	8.8	0.7 ± 0.3	0.9	1.1
	(6)	(1)	(4)	(2)	(2)
100% SW	5.7 ± 0.7	5.6	2.0 ± 0.6	1.9 ± 0.6	1.5
	(6)	(2)	(6)	(4)	(2)
10% SW	3.5 ± 0.3	4.7	2.4 ± 0.7	1.1 ± 0.2	-
	(5)	(2)	(4)	(4)	

* Values generally expressed as mean ± SE *(n)*, where *n* is the number of fish. Only washout space in 200% and 10% SW fish differed significantly ($P < 0.05$).

‡ Pooled values with irrigation media containing no K and 25 mM K.

FIGURE 8 Autoradiograph from 100% SW fish gill after 45 min of external irrigation with 50 μM ouabain (60 μCi/ml) and 25 min of additional irrigation without ouabain. This gill was perfused with ouabain-free medium during the entire 70 min. The underlying tissue section shows portions of two adjacent gill filaments. While there are few developed silver grains in the autoradiographic emulsion over the chloride cells of the upper filament, virtually every chloride cell is heavily labeled in the lower filament (part of spine showing). There is no accumulation of silver grains over the external surface of either filament. 1 μm section of freeze-dried, plastic-embedded tissue coated with a 2-μm layer of emulsion, exposed for 36 days, and photographed with phase-contrast optics. × 1,000.

certain filaments followed by limited dispersion via the contaminated perfusion flow; generalized leakage would have caused more uniform labeling of the chloride cells in adjacent filaments. Examination of irrigation-exposed filaments at higher magnification revealed no surface localization of autoradiographic grains associated with either pavement epithelial cells or apical crypt regions of chloride cells (Fig. 9). In fact, even in autoradiographs prepared before washout and with special dry-section modifications to further restrict [^{3}H]ouabain loss (see Materials and Methods) we never detected any grain localization over the crypt membrane (not shown). Moreover, the grain distribution pattern over those chloride cells which were labeled (Fig. 9) was similar to that observed over all chloride cells after vascular exposure (Fig. 7), i.e., the pattern paralleled the distribution of the tubular system. Thus, autoradiography after exposure of the external gill surface to ouabain supports localized leakage into interstitial fluid and provides no evidence for external ouabain binding sites.

Entry of Ouabain into Gills from the External Side

To further explore the nature of ouabain entry into gills from the external environment, we utilized two additional preparations, excised arches incubated in vitro and free-swimming fish in vivo. Simultaneous ouabain and inulin distribution

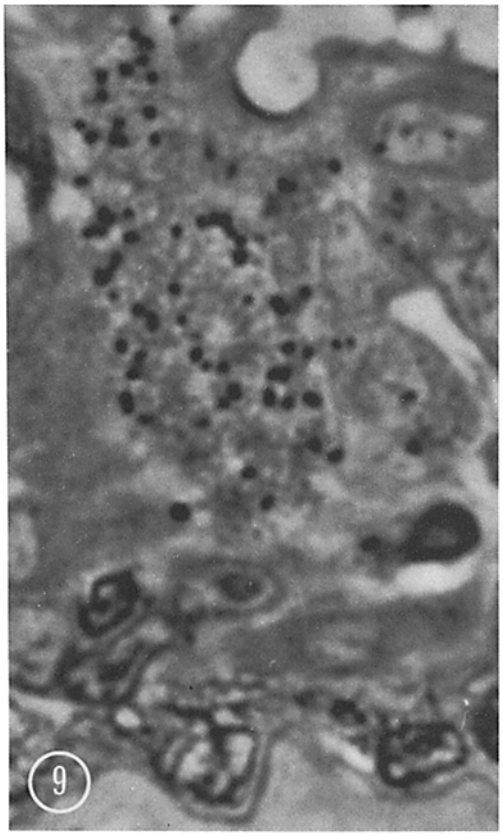

FIGURE 9 Autoradiograph from 100% SW fish gill exposed to [^{3}H]ouabain as in Fig. 8. The underlying tissue section shows a chloride cell with prominent apical crypt. The grain distribution pattern here, after external exposure to [^{3}H]ouabain, is similar (e.g., few silver grains adjacent to the apical crypt) to the pattern seen in chloride cells after vascular exposure (Fig. 7). No silver grains are associated with the apical crypt membrane. 1 μm section of freeze-dried, plastic-embedded tissue coated with a 2-μm layer of emulsion, exposed for 34 days, and photographed with phase-contrast optics. × 3,150.

spaces in these two preparations and the ouabain space in perfused-irrigated gills after 45 min of external exposure (no 25 min wash) are compared in Table IV. All data are for 100% SW fish. In excised gills incubated in vitro, 45 min was sufficient for the extracellular marker, inulin (mol wt ~5,000), to achieve a mean space value of 13.4% which is close to the typical whole fish extracellular space of 15% (above). For the same time period, the simultaneous ouabain (mol wt 584) space in excised gills was still larger, averaging 23.9%. Comparable space values were obtained when the external incubation medium consisted of 100% SW rather than 280 mM NaCl (Table IV, footnote). After subtraction of the inulin space, the remaining ouabain space gave a binding value of 7.3 μmol/kg gill filament, more than half that achieved after 45 min of vascular exposure (Table I, 100% SW fish). These results indicate that excised killifish gills are quite leaky to both inulin and ouabain. Even 5 min of external exposure produced detectable ouabain binding (Table IV). Qualitatively, our findings are like those of Maetz and Bornancin (28) who observed binding in excised eel gills exposed to 0.1 μM [^{3}H]ouabain for only 2 min.

In contrast to results with excised gills, external exposure of both perfused-irrigated gills and free-swimming fish gave small 45-min ouabain and inulin spaces (Table IV). Although excised gills incubated in vitro may be somewhat more leaky, constant removal of ouabain and inulin from gill interstitial fluid by the flow of vascular perfusate of blood probably explains the smaller space values under *in situ* and in vivo conditions. In fact, for free-swimming fish this explanation was verified by analyzing blood plasma and kidney, in addition to gills, after the 45 min of external exposure. The plasma contained finite concentrations of both ouabain and inulin (in each case about 0.4% of the corresponding concentration in the medium in which fish were swimming); the kidney had a ouabain distribution space which was half that for the gills (0.9 ± 0.2 SE percent kidney volume for the four fish) and an inulin space which was barely detectable (for purposes of comparison these in vivo distribution spaces in kidney, as in gill, are based on the concentrations in external medium rather than plasma). Clearly, in free-swimming killifish ouabain gained access into the circulatory system and was bound by another Na,K-ATPase-rich organ. In a similar experiment with free-swimming eels exposed for 1 h to potassium-free SW containing 100 μM ouabain, Silva et al. (45) observed inhibition of kidney as well as gill Na,K-ATPase. In conclusion, when molecules as large as inulin and ouabain are presented to the external surface of gills (in vitro, *in situ*, or in vivo), they apparently gain entry into the interstitial fluid through nonspecific leaks in the epithelium. Thus, external exposure almost certainly results in ouabain binding from interstitial fluid, e.g., at the tubular system membrane of chloride cells.

TABLE IV

[^{3}H]Ouabain and [^{14}C]Inulin Uptake from External Medium into Gill Filaments in Different Experimental Preparations with 100% SW-Adapted Killifish

Gill preparation	External medium‡	50 μM ouabain distribution space* (simultaneous inulin space)	
		5 min	45 min
		% gill arch volume	
Excised arch incubated in vitro	280 mM NaCl§	7.7 ± 1.0 (4.9 ± 0.9)	23.9 ± 2.6 (13.4 ± 1.3)
Perfused and irrigated *in situ*	280 mM NaCl	-	4.9 ± 1.5 (-)
Free-swimming fish in vivo	100% SW	-	1.9 ± 0.6 (1.2 ± 0.3)

* Apparent distribution volume based on concentration in external medium; values are mean ± SE, n = four fish.
‡ Contained 50 μM ouabain and in most experiments 10 mg% inulin.
§ Additional gill arches from each fish were incubated with 100% SW as the external medium; corresponding ouabain and inulin spaces were slightly larger in SW than in 280 mM NaCl, but the difference was generally not significant, i.e. $P > 0.05$.

DISCUSSION

The present study with perfused-irrigated gills from killifish adapted to environmental salinities ranging from 10% to 200% SW clearly establishes that almost all of the gill Na,K-ATPase is associated with the chloride cells and that the apparent subcellular location at all salinities is the extensively amplified basal and lateral cell surface facing interstitial fluid, i.e. the tubular system. Several lines of evidence support these conclusions. First, characterization experiments with 50 μM ouabain in the vascular perfusion medium demonstrated rapid and stable gill binding accompanied by essentially complete Na,K-ATPase inhibition at all salinities. Furthermore, the quantity of ouabain bound paralleled the increase in Na,K-ATPase activity in fish adapted to higher salinities. These findings offer convincing evidence for specific *in situ* binding of ouabain to gill Na,K-ATPase from the interstitial fluid side. In contrast, exposure of the external surface to 50 μM ouabain via the irrigation medium gave minimal and erratic results consistent with leakage of external ouabain into the interstitial fluid. Supplemental experiments with excised gills and free-swimming fish provided additional evidence for epithelial leaks large enough to pass inulin as well as ouabain. Second, [^{3}H]ouabain autoradiography at the cellular level clearly demonstrated that most of the gill binding was associated with chloride cells, irrespective of exposure or salinity. Moreover, the relative volume of these cells paralleled the increase in gill binding seen at higher salinities with vascular exposure. Given specific binding to the enzyme, these *in situ* findings define the chloride cell as the primary locus of adaptive Na,K-ATPase activity in killifish gills. Third, autoradiographic observations at the subcellular level revealed that the distribution pattern for the [^{3}H]ouabain bound to chloride cells was essentially identical to that for the tubular system, irrespective of salinity or exposure. Even with external exposure, no bound ouabain was detected at the apical crypt membrane. These observations support the conclusion that gill Na,K-ATPase is located primarily at the amplified interstitial fluid side (surface) of the chloride cells and that adaptive changes in enzyme activity reflect the quantity of tubular system membrane.

Localization of Na,K-ATPase to the amplified tubular system membrane is further supported by calculations involving the actual number of ouabain binding sites per chloride cell. Assuming one site for each molecule bound (16) and treating the chloride cell as a unit-density cylinder 20 μm long and 8 μm in diameter (Fig. 3), the measured concentration of 240 μmol ouabain/kg cell (Table II) gives 1.5×10^8 sites/cell in 100% SW-adapted fish. This number is large, e.g., when compared to 6×10^4 ouabain sites/fish erythrocyte (5), and even if uniformly distributed over the whole unamplified surface of the above cylinder, i.e., over

an area of 6×10^{10} Å^2, would constitute one site for each 400 Å^2 of surface. Since both particle size and molecular weight estimates for semipurified Na,K-ATPase (7) are consistent with each enzymatic site occupying at least 1,000 Å^2 of membrane, surface amplification appears to be a prerequisite for accommodation of the large number of sites associated with each chloride cell. For example, if the tubular system constitutes a 100-fold amplification of the cell surface, there would be 40,000 Å^2 of membrane for each ouabain binding site, an area which compares favorably with those of 10,000 and 50,000 Å^2 estimated for frog choroid plexus (35) and squid giant axon (2), respectively. Finally, if Na,K-ATPase sites are spaced this far apart, i.e. one per 40,000 Å^2, it can be calculated that the apical crypt membrane could accommodate only a very small percentage of the total Na,K-ATPase associated with each chloride cell. For example, a spherical crypt 3 μm in diameter (Fig. 6) would accommodate 7.5×10^4 sites or only 0.05% of the total per chloride cell in 100% SW fish. Clearly, such a small number of apical sites would be undetectable (Fig. 9), and their existence can be neither affirmed nor denied on the basis of present autoradiographs.

The only previous attempts at subcellular localization of chloride cell Na,K-ATPase are three cytochemical studies in which the highly criticized, Wachstein-Meisel Pb-capture reaction was used (12, 31, 44) and a low-resolution autoradiographic study with [^{3}H]ouabain (unpublished work by Masoni and Bornancin cited in reference 28). Gill tissue for these studies was generally obtained from eels adapted to SW. Although the latter two cytochemical studies demonstrated ATPase reaction product associated with both the tubular system and the apical region, this localization cannot be considered specific for Na,K-ATPase because the reaction was not ouabain sensitive. For an objective evaluation of ATPase cytochemistry and other localization techniques, see Schwartz et al. (43). In the autoradiographic study on excised gills incubated in ouabain-containing medium, the resolution is too low to permit any conclusions about ouabain binding sites at the apical crypt membrane. Interestingly, however, in these autoradiographs, as in low magnification views of our external exposure autoradiographs, the silver grains appeared to be distributed rather uniformly over the whole area occupied by each chloride cell. Since the excised gills were incubated with ouabain for only 2–5 min, Maetz and Bornancin (28) contend that ouabain penetrated deep into the chloride cells directly from the apical crypt. A more likely explanation is binding at tubular system sites secondary to rapid leakage of ouabain into gill interstitial fluid. For example, we have demonstrated measurable inulin as well as ouabain distribution spaces in excised killifish gills incubated for 5 min (Table IV). Furthermore, there are several reports of organic molecules, including inulin, being lost from plasma across the gill epithelium (23, 29) and, although such molecules accumulate in chloride cells (29), it seems more reasonable that transepithelial leakage occurs primarily in the respiratory portion of the gill, i.e. in the lamellae which account for most of the surface area. In any case, ouabain clearly penetrates from external media into the blood vascular system of free-swimming fish (Table IV) (45) and claims that this inhibitor acts at the external side of the gill (13, 34) must be accompanied by evidence that ouabain molecules have not gained access to the interstitial fluid and, hence, the tubular system Na,K-ATPase.

The final question to be considered is the role of tubular system Na,K-ATPase in chloride cell function. In single cell systems such as erythrocyte and nerve, the site of ouabain action is the external side of the plasma membrane, i.e. the surface to which the Na is actively transported (7, 16, 43). In epithelia responsible for salt absorption, e.g., rabbit intestine (47) and frog bladder (30), or salt secretion, e.g., frog choroid plexus (35), well-controlled [^{3}H]ouabain autoradiography has consistently demonstrated binding sites (Na,K-ATPase) at the pole of the epithelial cell from which Na is actively transported, i.e. the basal-lateral surface in the absorbing systems and the apical surface in the secreting system. Thus, basal-lateral localization of Na,K-ATPase in chloride cells implies that Na is actively transported from these cells into interstitial fluid. While this pump orientation seems reasonable for chloride cells functioning as absorbing cells in fish adapted to salinities less than that of their plasma, e.g., to FW or 10% SW, it represents a paradox for chloride cells functioning as secreting cells in high salinity environments, e.g., 100% or 200% SW, since Na would be pumped into rather than out of the fish. In fact, Maetz's long-standing model of the chloride cell (27, 28) has the Na,K-ATPase, which is postulated as being responsible for Na secretion, located at the apical crypt membrane. While our autoradiographs neither confirm nor exclude a

small number of enzyme sites at this membrane, the large increase in Na,K-ATPase activity accompanying adaptation to high salinity is clearly associated with some other part of the cell, most probably the tubular system membrane. As early as 1972, Motais and Garcia-Romeu (32) surmised that most gill Na,K-ATPase was associated with the tubular system and suggested that its function in high salinity environments was solute recycling and water absorption rather than active Na secretion. Moreover, Kirschner et al. (22) have now concluded on the basis of available electrophysiological data that the primary osmoregulatory mechanism in gills of SW-adapted fish is a secretory Cl pump and that it may not even be necessary to postulate a secretory Na pump.

Clearly, further investigation will be required to clarify the enigmatic role of tubular system Na,K-ATPase in chloride cell function. It is also important to recognize that this enigma extends to other extrarenal osmoregulatory organs, such as avian and reptilian nasal glands, whose principal salt-secreting cells likewise possess an enormously amplified basal-lateral surface. With a ouabain-sensitive cytochemical reaction (Ernst *p*-nitrophenyl phosphate-hydrolysis), this surface has recently been shown to be the major site of Na,K-ATPase activity in the nasal salt gland of both a bird (10) and a lizard (8). Localization of the enzyme activity at this surface is consistent with Na being pumped from the cells into interstitial fluid. Consequently, as in chloride cells of SW-adapted fish, the basal-lateral pump appears to be oriented in the wrong direction for removing Na from the organism. Perhaps, as Peaker and Linzell (33) have suggested for the avian salt gland, basal-lateral Na,K-ATPase plays a primary role in regulation of intracellular ion concentrations and, hence, only a secondary role in net salt secretion. In chloride cells of FW-adapted fish, however, this enzyme could also assume a primary role in net salt absorption. Thus, basal-lateral Na,K-ATPase might contribute both indirectly and directly to the dual secretory-absorptive faculty of the euryhaline teleost gill.

The authors thank Mr. Harold Church and Miss Sharon Bowes for their excellent technical assistance.

Preliminary aspects of this work were reported in Stirling, C. E., K. J. Karnaky, Jr., L. B. Kinter, and N. B. Kinter. 1973. *Bull. Mt. Desert Island Biol. Lab.* **13:**117–120. and Stirling, C. E., L. B. Kinter, K. J. Karnaky, Jr., and W. B. Kinter. 1974. *Fed. Proc.* **33:**207.

This investigation was supported by Public Health Service Grants AM 15973 to William B. Kinter and AM 13182 to Charles E. Stirling and Fellowship GM 57244 to Karl J. Karnaky, Jr.

Received for publication 21 August 1975, and in revised form 4 February 1976.

REFERENCES

1. Baker, P. F. 1972. The sodium pump in animal tissues and its role in the control of cellular metabolism and function. *In* Metabolic Pathways. Vol. VI. Metabolic Transport. L. E. Hokin, editor. Academic Press, Inc., New York. 243–268.
2. Baker, P. F., and J. S. Willis. 1972. Inhibition of the sodium pump in squid giant axons by cardiac glycosides: dependence on extracellular ions and metabolism. *J. Physiol.* **224:**463–475.
3. Bergman, H. L., K. R. Olson, and P. O. Fromm. 1974. The effects of vasoactive agents on the functional surface area of isolated-perfused gills of rainbow trout. *J. Comp. Physiol.* **94:**267–286.
4. Bonting, S. L. 1970. Sodium-potassium activated adenosine triphosphatase and cation transport. *In* Membranes and Ion Transport. Vol. 1. Ch. 8. E. E. Bittar, editor. John Wiley & Sons, Inc., New York. 257–363.
5. Cala, P. M. 1974. Volume regulation by flounder *(Pseudopleuronectes americanus)* red blood cells in anisotonic media. Doctoral Dissertation, Case Western Reserve University, Cleveland, Ohio.
6. Copeland, D. E. 1948. The cytological basis of chloride transfer in the gills of *Fundulus heteroclitus*. *J. Morphol.* **82:**201–227.
7. Dahl, J. L., and L. E. Hokin. 1974. The sodium-potassium adenosine-triphosphatase. *Annu. Rev. Biochem.* **43:**347–356.
8. Ellis, R. A., and C. C. Goertemiller, Jr. 1974. Cytological effects of salt-stress and localization of transport adenosine triphosphatase in the lateral nasal glands of the desert iguana, *Dipsosaurus dorsalis*. *Anat. Rec.* **180:**285–297.
9. Epstein, F. H., A. I. Katz, and G. E. Pickford. 1967. Sodium- and potassium-activated adenosine triphosphatase of gills: Role in adaptation of teleosts to salt water. *Science (Wash. D. C.).* **156:**1245–1247.
10. Ernst, S. A. 1972. Transport adenosine triphosphatase cytochemistry. II. Cytochemical localization of ouabain-sensitive, potassium-dependent phosphatase activity in the secretory epithelium of the avian salt gland. *J. Histochem. Cytochem.* **20:**23–38.
11. Ernst, S. A., C. C. Goertemiller, Jr., and R. A. Ellis. 1967. The effect of salt regimens on the development of (Na-K)-dependent ATPase activity during growth of salt glands of ducklings. *Biochim. Biophys. Acta.* **135:**682–692.

12. ERNST, S. A., and C. W. PHILPOTT. 1970. Preservation of Na-K-activated and Mg-activated adenosine triphosphatase activities of avian salt gland and teleost gill with formaldehyde as fixative. *J. Histochem. Cytochem.* **18:**251-263.
13. EVANS, D. H., C. H. MALLERY, and L. KRAVITZ. 1973. Sodium extrusion by a fish acclimated to sea water: physiological and biochemical description of a Na-for-K exchange system. *J. Exp. Biol.* **58:**627-636.
14. FORREST, J. N., JR., A. D. COHEN, D. A. SCHON, and F. H. EPSTEIN. 1973. Na transport and Na-K-ATPase in gills during adaptation to seawater: effects of cortisol. *Am. J. Physiol.* **224:**709-713.
15. FORSTER, R. P. 1948. Use of thin kidney slices and isolated renal tubules for direct study of cellular transport kinetics. *Science (Wash. D. C.).* **108:**65-67.
16. GLYNN, I. M., and S. J. D. KARLISH. 1975. The sodium pump. *Annu. Rev. Physiol.* **37:**13-55.
17. GOMORI, G. 1955. Preparation of buffers for use in enzyme studies. *In* Methods in Enzymology. Vol. I. S. P. Colowich and N. O. Kaplan, editors. Academic Press, Inc., New York. 138-146.
18. HOLMES, W. N., and E. M. DONALDSON. 1969. The body compartments and the distribution of electrolytes. *In* Fish Physiology. Vol. I. Excretion, Ionic Regulation, and Metabolism. W. S. Hoar and D. J. Randall, editors. Academic Press, Inc., New York. 1-89.
19. KAMIYA, M. 1972. Sodium-potassium-activated adenosinetriphosphatase in isolated chloride cells from eel gills. *Comp. Biochem. Physiol.* **43 B:**611-617.
20. KARNAKY, K. J., JR., S. A. ERNST, and C. W. PHILPOTT. Teleost chloride cell. I. Response of pupfish *(Cyprinodon variegatus)* gill Na,K-ATPase and chloride cell fine structure to various high salinity environments. *J. Cell Biol.* **70:**144-156.
21. KIRSCHNER, L. B. 1969. Ventral aortic pressure and sodium fluxes in perfused eel gills. *Am. J. Physiol.* **217:**596-604.
22. KIRSCHNER, L. B., L. GREENWALD, and M. SANDERS. On the mechanism of sodium extrusion across the irrigated gill of sea water-adapted rainbow trout *(Salmo gairdneri). J. Gen. Physiol.* **64:**148-165.
23. LAM, T. J. 1969. Evidence of loss of ^{14}C-inulin via the head of the three spine stickleback, *Gasterosteus aculeatus,* form *trachurus. Comp. Biochem. Physiol.* **28:**459-463.
24. LOWRY, O. H., N. J. ROSEBROUGH, A. L. FARR, and R. J. RANDALL. 1951. Protein measurement with the Folin phenol reagent. *J. Biol. Chem.* **193:**265-275.
25. LUFT, J. H. 1961. Improvements in epoxy resin embedding methods. *J. Biophys. Biochem. Cytol.* **9:**409-414.
26. MAACK, T., D. D. S. MACKENSIE, and W. B. KINTER. 1971. Intracellular pathways of renal reabsorption of lysozyme. *Am. J. Physiol.* **221:**1609-1616.
27. MAETZ, J. 1971. Fish gills: mechanisms of salt transfer in fresh water and sea water. *Philos. Trans. R. Soc. Lond. B Biol. Sci.* **262:**209-249.
28. MAETZ, J., and M. BORNANCIN. 1975. Biochemical and biophysical aspects of salt excretion by chloride cells in teleosts. *Fortschr. Zool.* **23**(2/3):322-362.
29. MASONI, A., and P. PAYAN. 1974. Urea, inulin and para-amino-hippuric acid (PAH) excretion by the gills of the eel, *Anguilla anguilla* L. *Comp. Biochem. Physiol.* **47 A:**1241-1244.
30. MILLS, J. W., and S. A. ERNST. 1975. Localization of sodium pump sites in frog urinary bladder. *Biochim. Biophys. Acta.* **375:**268-273.
31. MIZUHIRA, V., T. AMAKAWA, S. YAMASHINA, N. SHIRAI, and S. VTIDA. 1970. Electron microscopic studies on the localization of sodium ions and sodium-potassium-activated adenosine triphosphatase in chloride cells of eel gills. *Exp. Cell. Res.* **59:**346-348.
32. MOTAIS, R., and F. GARCIA-ROMEU. 1972. Transport mechanisms in the teleostean gill and amphibian skin. *Annu. Rev. Physiol.* **34:**141-176.
33. PEAKER, M., and J. LINZELL. 1975. Salt Glands in Birds and Reptiles. Cambridge University Press, Cambridge. Ch. 6.
34. MOTAIS, R., and J. ISAIA. 1972. Evidence for an effect of ouabain on the branchial sodium-excreting pump of marine teleosts: interaction between the inhibitor and external Na and K. *J. Exp. Biol.* **57:**367-373.
35. QUINTON, P. M., E. M. WRIGHT, and J. McD. TORMEY. 1973. Localization of sodium pumps in the choroid plexus epithelium. *J. Cell Biol.* **58:**724-730.
36. RANKIN, J. C., and J. MAETZ. 1971. A perfused teleostean gill preparation: vascular actions of neurohypophysial hormones and catecholamines. *J. Endocrinol.* **51:**621-635.
37. REYNOLDS, E. S. 1963. The use of lead citrate at high pH as an electron-opaque stain in electron microscopy. *J. Cell Biol.* **17:**208-212.
38. RICHARDSON, K. C., L. JARRETT, and E. H. FINKE. 1960. Embedding in epoxy resins for ultrathin sectioning in electron microscopy. *Stain Technol.* **35:**313-323.
39. RITCH, R., and C. W. PHILPOTT. 1969. Repeating particles associated with an electrolyte-transport membrane. *Exp. Cell Res.* **55:**17-24.
40. SARGENT, J. R., and A. J. THOMSON. 1974. The nature and properties of the inducible sodium-plus-potassium ion-dependent adenosine triphosphatase in the gills of eels *(Anguilla anguilla)* adapted to fresh water and sea water. *Biochem. J.* **144:**69-75.
41. SARGENT, J. R., A. J. THOMSON, and M. BORNANCIN. 1975. Activities and localization of succinic

dehydrogenase and Na^+/K^+-activated adenosine triphosphatase in the gills of fresh water and sea water eels *(Anguilla anguilla)*. *Comp. Biochem. Physiol.* **51 B:**75–79.

42. SCHMIDT-NIELSEN, B. 1974. Osmoregulation: effect of salinity and heavy metals. *Fed. Proc.* **33:**2137–2146.
43. SCHWARTZ, A., G. E. LINDENMAYER, and J. C. ALLEN. 1975. The sodium-potassium adenosine triphosphatase: pharmacological, physiological and biochemical aspects. *Pharmacol. Rev.* **27:**3–134.
44. SHIRAI, N. 1972. Electron microscope localization of sodium ions and adenosinetriphosphatase in chloride cells of the Japanese eel, *Anguilla japonica*. *J. Fac. Sci. Univ. Tokyo. Sec. IV.* **12:**385–403.
45. SILVA, P., F. H. EPSTEIN, K. SPOKES, S. EPSTEIN, and R. SOLOMON. 1974. Quantitative aspects of the inhibition of gill Na-K-ATPase by internal and external ouabain in seawater eels, *Anguilla rostrata*. *Bull. Mt. Desert Island Biol. Lab.* **14:**119–122.
46. SKADHAUGE, E. 1969. The mechanism of salt and water absorption in the intestine of the eel *(Anguilla anguilla)* adapted to waters of various salinities. *J. Physiol.* **204:**135–158.
47. STIRLING, C. E. 1972. Radioautographic localization of sodium pump sites in rabbit intestine. *J. Cell Biol.* **53:**704–714.
48. STIRLING, C. E., and W. B. KINTER, 1967. High-resolution radioautography of galactose-^3H accumulation in rings of hamster intestine. *J. Cell Biol.* **35:**585–604.
49. ZAUGG, W. S., and L. R. MCLAIN. 1971. Gill sampling as a method of following biochemical changes: ATPase activities altered by ouabain injection and salt water adaption. *Comp. Biochem. Physiol.* **38 B:**501–506.